[redacted]

OFFICE OF SCIENTIFIC RESEARCH & DEVELOPMENT
NATIONAL DEFENSE RESEARCH COMMITTEE.
DIVISION SIX-SECTION 6.1

# WATER TUNNEL TESTS
OF THE
# 2¼" AA ROCKET PROJECTILE



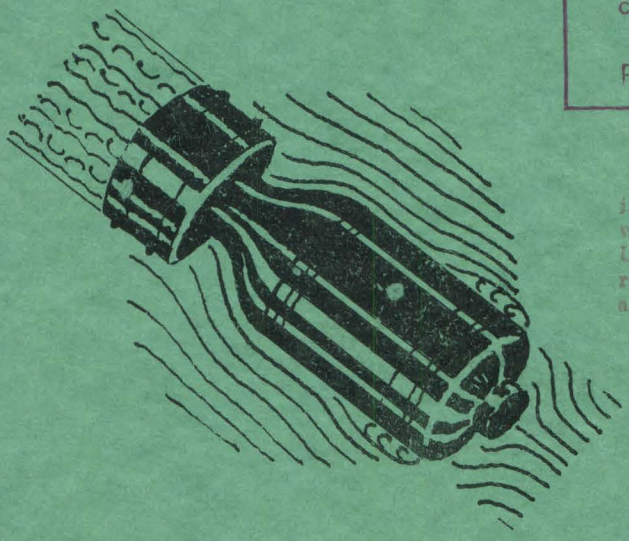



FILE COPY

THE HIGH SPEED WATER TUNNEL
CALIFORNIA INSTITUTE OF TECHNOLOGY
PASADENA, CALIFORNIA.

SECTION No 6-1-SR-207-927

REPORT N.D. 13.1

COPY No 101

[redacted]

~~(CONFIDENTIAL)~~

OFFICE OF SCIENTIFIC RESEARCH AND DEVELOPMENT
NATIONAL DEFENSE RESEARCH COMMITTEE
DIVISION SIX — SECTION 6.1

# WATER TUNNEL TESTS OF THE 2 1/4" AA ROCKET PROJECTILE

BY

ROBERT T. KNAPP
OFFICIAL INVESTIGATOR

THE HIGH SPEED WATER TUNNEL
AT THE
CALIFORNIA INSTITUTE OF TECHNOLOGY
HYDRAULIC MACHINERY LABORATORY
PASADENA, CALIFORNIA

Section No. 6.1-sr-207-927
HML Rep. No. ND-13.1

Report Prepared By:
James W. Daily
Hydraulic Engineer

December 28, 1943

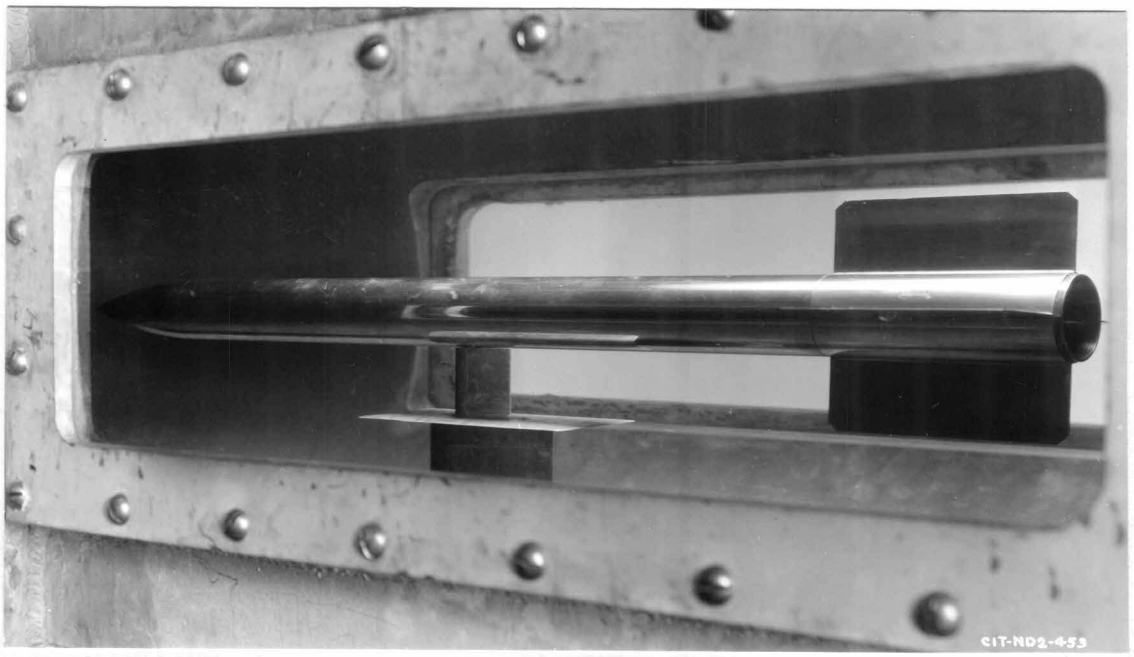


FIGURE 1
1 1/2" DIAMETER MODEL OF THE 2 1/4" AA ROCKET PROJECTILE
MOUNTED IN WATER TUNNEL AS VIEWED THROUGH
THE TRANSPARENT SIDE WINDOWS OF THE WORKING SECTION.

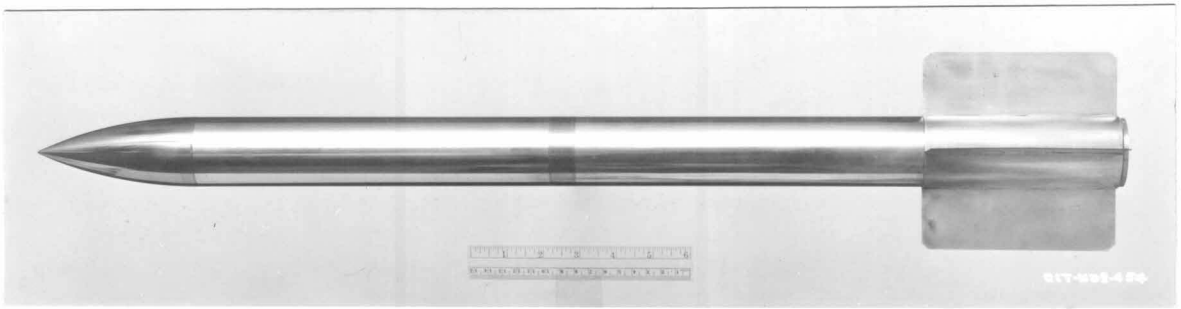

FIGURE 2
2" DIAMETER MODEL OF THE 2 1/4" AA ROCKET PROJECTILE.

# ABSTRACT

The High Speed Water Tunnel is operated by the California Institute of Technology under Contract OEMsr-207 with the Office of Scientific Research and Development, and is sponsored by Division Six, Section 6.1, of the National Defense Research Committee.

The report covers Water Tunnel tests of 1-1/2" and 2" diameter models of the 2-1/4" AA Rocket Projectile. The drag, cross force, and moment acting on the models were measured and the position of the center of pressure relative to the center of gravity was calculated for various yaw angles. These results were compared with prototype field test data.

The main findings are summarized as follows:

1. The rocket is statically stable as indicated by a stabilizing moment coefficient and a center-of-pressure eccentricity of more than 0.26. Furthermore, the large area of the tail fins will probably provide sufficient damping to make it dynamically stable also.
2. The tail fins cause very large cross force coefficients compared to values for other cylindrical projectiles with folding fin or ring tails. Consequently, unless the rocket is rotated in flight, small misalignments of the tail fins can cause drifting and increase the dispersion seriously.
3. Both the cross force and moment coefficients increase with yaw at a greater than linear rate.
4. Comparison of Water Tunnel and field test data shows good agreement for the moment coefficient.
5. The drag coefficient from Water Tunnel tests is 9% lower than the value of 0.46 measured during field tests in air. Scale effects, oscillation of the projectile during free flight tests, and compressibility effects on the drag in air are factors that could account for this difference.
6. The drag is nearly independent of yaw for small angles and increases rapidly for angles greater than about $4^{\circ}$.
7. The high drag coefficient for this projectile is caused by skin friction on the relatively large area of the body and fins and by pressure drag due primarily to a large eddying wake behind the blunt body.

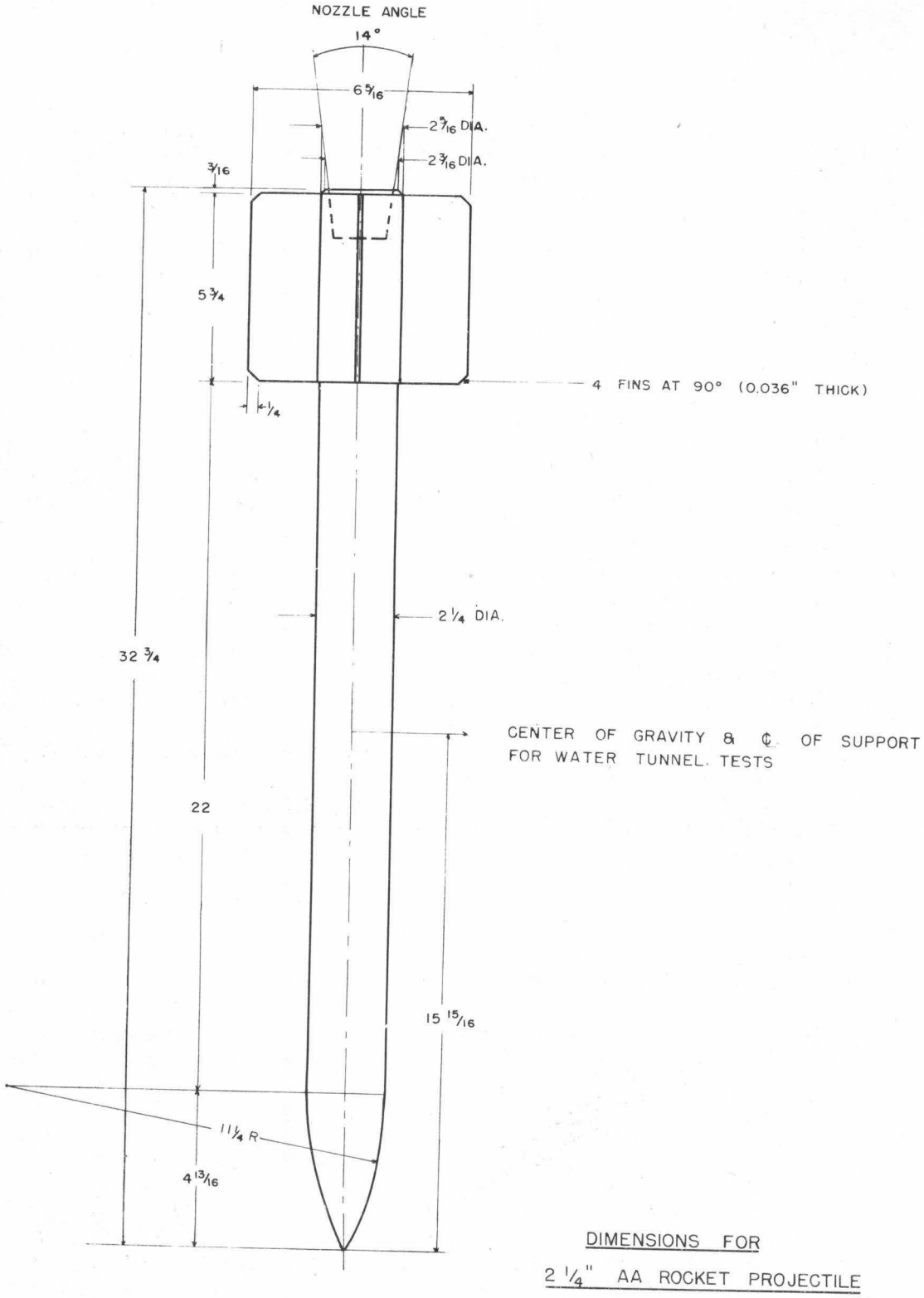


DIMENSIONS FOR
2 1/4" AA ROCKET PROJECTILE

CIT — HML
DRG. ND - 574 - U



FIGURE 3

## I. PURPOSE OF TESTS

This report describes the results of Water Tunnel tests of 1-1/2" and 2" diameter models of the 2-1/4" AA Rocket Projectile. The purpose of the tests was to measure the hydrodynamic drag, cross force, and moment acting on the projectile for different angles of yaw with respect to the flow, and to determine the position of the center of pressure relative to the center of gravity of the projectile.

## II. DESCRIPTION OF PROJECTILE AND TEST INSTALLATION

Figure 1 shows the 1-1/2" diameter model of the rocket installed in the Water Tunnel working section ready for test. The projectile is made up of a 5 caliber radius ogive nose and a long cylindrical body to which are attached four large tail fins. Figure 2 shows a profile of the 2" diameter model. Outline dimensions of the full-scale projectile are shown in Figure 3. Observe that the center of gravity of this projectile is at a point 49% of the overall length back from the nose.

The tests were conducted in the 14" diameter working section of the High Speed Water Tunnel at the California Institute of Technology. Details of the Water Tunnel are described in Appendix A and in reference (1) listed at the end of this report. As described there and as shown in Figure 1, a shield, which projects up to within a few thousandths of an inch of the projectile, is used to protect the spindle from the flow so as to eliminate tare corrections. So as to measure the support interference effects, tests were also made with an image of this shield placed above the model. This image shield also projected to within a few thousandths of an inch of the projectile, but did not touch it.

The Water Tunnel measurements, when corrected for interference and other effects, give results which are applicable either in water or in air at velocities up to about 700 feet per second. For velocities near or above sonic the results will not apply.

## III. PRESENTATION OF TEST DATA

Preliminary measurements of the characteristics of the 2-1/4" AA projectile were made with the 2" diameter model. Because of the length and the spread of the large tail fins, the yaw angles for tests were limited if the water tunnel wall was not to be approached so closely as to introduce undesirable effects. In addition, the hydrodynamic forces and moments caused the model to oscillate and vibrate severely at high speeds, making accurate measurements difficult. Consequently, the 1-1/2" diameter model was constructed and supplementary tests were made using it.

Figure 4 shows curves of drag, cross force, and moment coefficients and center-of-pressure eccentricity that were derived from tests of both models. Definitions of the terms and symbols used to present the

data are given in Appendix B. For the zero to 5° yaw angle range the curves are from tests of the 2" diameter model at a velocity of 14.4 feet per second or at a Reynolds number of 3,000,000 based on the projectile length. The Reynolds number for the full-scale projectile in free flight is about 10,900,000. Beyond 5° yaw the curves were extrapolated using data from tests of the 1-1/2" diameter model. These data have been corrected for interference effects and apply to the projectile in free flight. The uncertainties introduced by the extrapolation and interference correction procedures at the larger yaw angles are estimated to be not more than 10%. Figure 6 shows the variation of drag with Reynolds number obtained from tests of the 2" diameter model. These data have also been corrected for interference effects.

## IV. MOMENT COEFFICIENT AND STABILITY

The moment coefficient and center-of-pressure eccentricity curves in Figure 4 show that this rocket is stable. The moment coefficient is stabilizing over the entire yaw range of the tests. Furthermore, the "stiffness", or tendency to resist further yawing, as shown by the slope of the coefficient curve, increases continuously with yaw. The resulting CP eccentricity varies from 0.26 at 1° yaw to 0.28 at 12° yaw. The moment coefficient and the eccentricity are measures of the "static" stability, i.e. the forces acting on the projectile to return to its equilibrium orientation with respect to the line of flight after a disturbance. They do not describe the dynamic stability, the tendency of any oscillatory motion to subside. The dynamic stability will depend upon the degree of damping which the projectile undergoes as it oscillates. In air the damping in general is small but it is probable that the large fin area of this projectile will provide sufficient damping to assure reasonable dynamic stability.

## V. COMPARISON OF WATER TUNNEL AND FIELD TEST MOMENT COEFFICIENTS

The moment coefficients obtained from Water Tunnel tests can be compared with field test data by means of the following relationship:

$$M = C_M \rho \frac{V^2}{2} AL = 4\pi^2 V^2 I \frac{\Psi}{\sigma^2} \qquad (1)$$

This reduces to

$$\sigma = \frac{10}{d} \sqrt{\frac{I}{C_M/\Psi \rho L}} \qquad (1a)$$

or

$$C_M/\Psi = \frac{32\pi I}{d^2 \rho L \sigma^2} \qquad (1b)$$

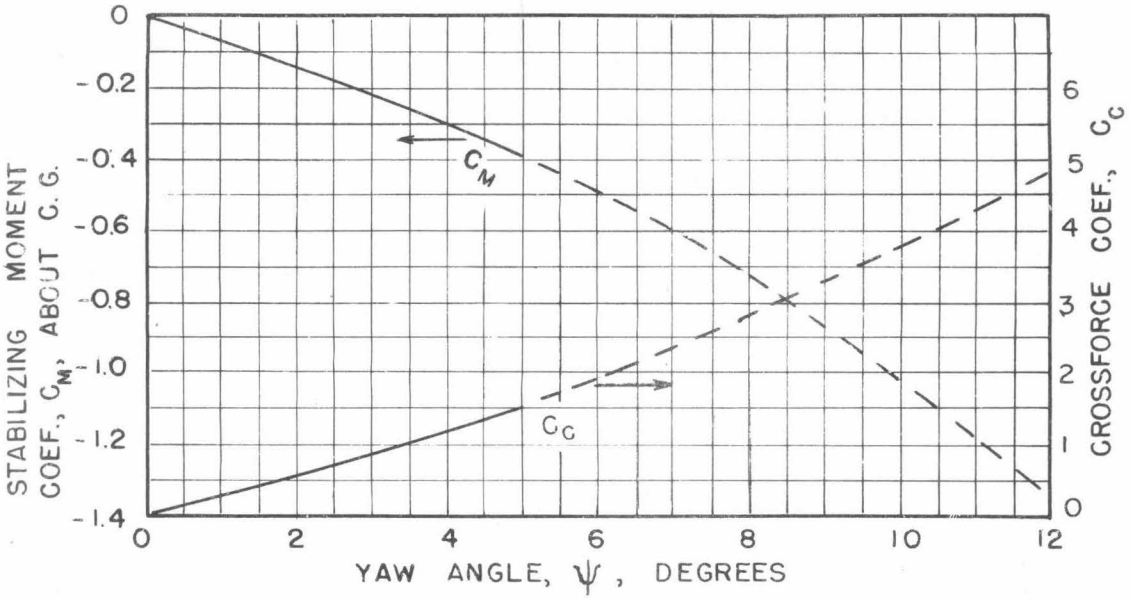


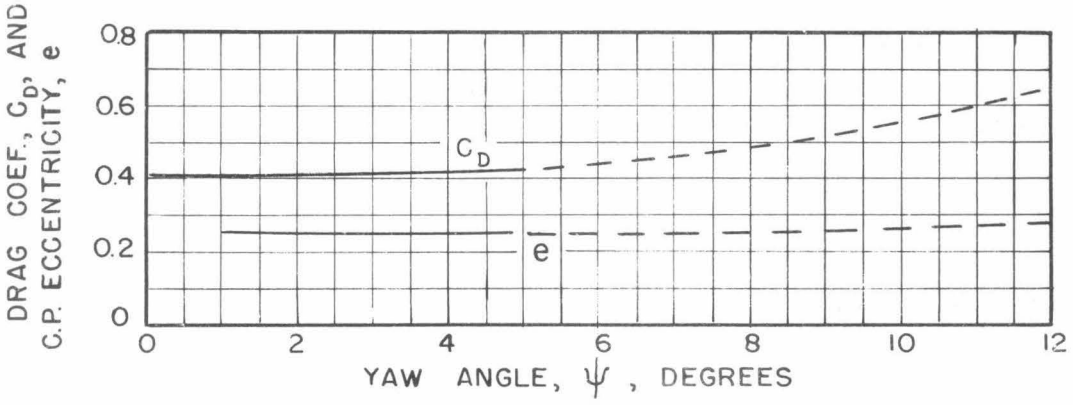


# $2\frac{1}{4}$" AA ROCKET PROJECTILE

DRAG, CROSSFORCE, AND MOMENT COEFFICIENTS
AND CENTER OF PRESSURE ECCENTRICITY
FROM WATER TUNNEL TESTS
OF $1\frac{1}{2}$" & 2" DIAMETER MODELS
AT R = 3,000,000

CIT — HML
RUNS 4 – 15
SHEET ND 13-1854L

FIGURE 4

where in addition to the quantities defined in Appendix B, I is the transverse moment of inertia in slug-ft$^2$ of the projectile taken about the center of gravity, and $\sigma$ is the distance in feet that the projectile travels in free flight during one oscillation.

The right-hand expression in equation (1) is obtained by assuming, as a first approximation, that a projectile oscillating in free flight undergoes simple harmonic motion (zero damping). By means of this relationship it is possible to compare values of $\sigma$, the primary experimental quantity from free flight tests in air, with $C_M/\psi$, the average slope of the moment coefficient curve obtained from Water Tunnel tests. The comparison made in the following table is based on free flight test data supplied by the California Institute of Technology OSRD Rocket Group[2] and Water Tunnel data from Figure 4.

TABLE I

COMPARISON OF WATER TUNNEL AND FIELD TEST DATA

| Test Location | Amplitude of Oscillation $\psi$, degrees | Length of Oscillation $\sigma$, feet | Moment Coef. Per Radian of Yaw $C_M/\psi$ | Reynolds Number R |
|---|---|---|---|---|
| Test Range | 5 (measured) | 164 (Measured) | 4.4 | 10,900,000 |
| Water Tunnel | 5 (assumed) | 168 | 4.5 (Measured) | 3,000,000 |
| Water Tunnel | 8 " | 153 | 5.2 " | 3,000,000 |
| Water Tunnel | 12 " | 141 | 6.4 " | 3,000,000 |

The first two lines show remarkable agreement of the Water Tunnel and field test data. The last two lines show the effect of the increased "stiffness" encountered with higher amplitudes on the length of oscillation.

All the tests reported in Figure 4 and represented in the above tabulation were made with the rocket tail fins in vertical and horizontal planes as shown in Figure 1. Tests made with the fins rotated 45° gave values of $C_M$ (and $C_C$) approximately 10% higher than shown in Figure 4.

## VI. CROSS FORCE COEFFICIENT AND ACCURACY

The cross force coefficient curve for this rocket is steep at zero yaw and increases with yaw at a greater than linear rate to a value of 4.7 at 12° yaw. This value, which is probably caused by the large tail fin area, may be compared with values of the order of 1.0 at the same yaw for other cylindrical projectiles with either folding fin or ring tails. This powerful effect is very important because small misalignments of the tail surfaces, unless the rocket is purposely rotated during flight, may cause serious drifting from the set course.

(2) Figures refer to references listed at the end of this report.

The following tabulation shows estimates of the possible dispersion for the field test conditions already mentioned and an assumed 3,000 yard range to be as high as 70 mils for a one-half degree misalignment of one pair of fins. These estimates assume no rotation of the projectile.

TABLE II

ESTIMATED DISPERSION DUE TO TAIL FIN MISALIGNMENTS

| Fin Misalignment In Degrees | Range In Yards (Assumed) | Drift from Original Course In Feet | Equivalent Dispersion In Mils |
|---|---|---|---|
| 1/4 | 1000 | 34.8 | 11.6 |
| 1/4 | 3000 | 313 | 35 |
| 1/2 | 1000 | 69.6 | 23.2 |
| 1/2 | 3000 | 625 | 70 |

On the other hand, the effect of the cross force in displacing the rocket laterally during a part of an oscillation will have no significant effect on the accuracy. The maximum lateral displacement from this course is calculated to be only about a tenth of a foot, a negligible amount.

## VII. DRAG — VARIATION WITH YAW AND COMPARISON WITH FULL-SCALE TEST DATA

Figure 4 shows that the drag coefficient of the 2-1/4" AA projectile is nearly independent of yaw for small angles, but increases appreciably for larger angles, say above $3^{\circ}$ or $4^{\circ}$. The measured drag coefficient at zero yaw is 0.42 at a Reynolds number of 3,000,000. The full-scale deceleration test of the projectile in air gave a value of 0.46 for R = 10,900,000, a discrepancy of only 9%. There are several factors that might contribute to this 9% difference, in addition to inherent inaccuracies in both test procedures. First, there are "scale effects" due to difference in Reynolds number, relative roughness of projectiles, and relative turbulence levels of the media surrounding the projectiles. Second, there are the effects of oscillations during the field deceleration tests on the drag. Third, there are the effects of compressibility on the drag of the body and fins during flight in air.

The magnitude of the scale effects is obtained by comparing variable velocity Water Tunnel runs of the 2" diameter model with and without a "spoiler" wire band around the nose located as shown in Figure 5. The spoiler wire assures a completely turbulent boundary layer on the model at all test Reynolds numbers and thus simulates a condition that is probably also caused on the prototype by construction joints between nose and body. Since both the prototype and model are otherwise smooth, the tests with the spoiler should give $C_D$ = 0.46 unless other factors in addition to scale effects cause differences in the Water Tunnel and full scale tests. The results of these tests are both shown in Figure 6 as $C_D$ vs. Reynolds number on a log log diagram. Without the spoiler wire the Water Tunnel measurements give a constant $C_D$ of 0.42 over the entire Reynolds number range probably indicating that a transition is occurring between laminar and turbulent boundary layers. With the spoiler wire $C_D$ decreases from 0.53 at R = 1,800,000 to 0.435 at R = 10,000,000, showing a typical trend for a completely turbulent boundary layer, but still leaving $C_D$ at full scale R 5% less than obtained in the field.

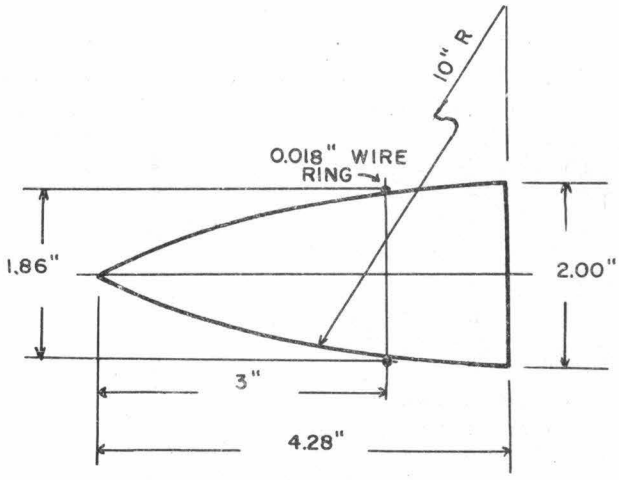


FIGURE 5
LOCATION OF SPOILER RING
ON 2" DIAMETER MODEL

During field tests the projectile was observed to oscillate about its center of gravity through a yaw angle of about $\pm$ 5°. As the curves in Figure 4 show, $C_D$ at 5° is about 2.5% higher than at zero degrees. Furthermore, it is quite probable that the energy consumed by the oscillating projectile is greater than that measured by the steady state Water Tunnel tests. It is thought that the total effect of the oscillations could account for the remaining difference between full scale and model drag measurements.

The final item of compressibility that might effect the full-scale drag measurements depends on the Mach number for the free flight conditions. The velocity of the rocket in air is 680 feet per second, which gives a Mach number of about 0.63. While this is below the range of compressibility effects for many projectile shapes, NACA tests of

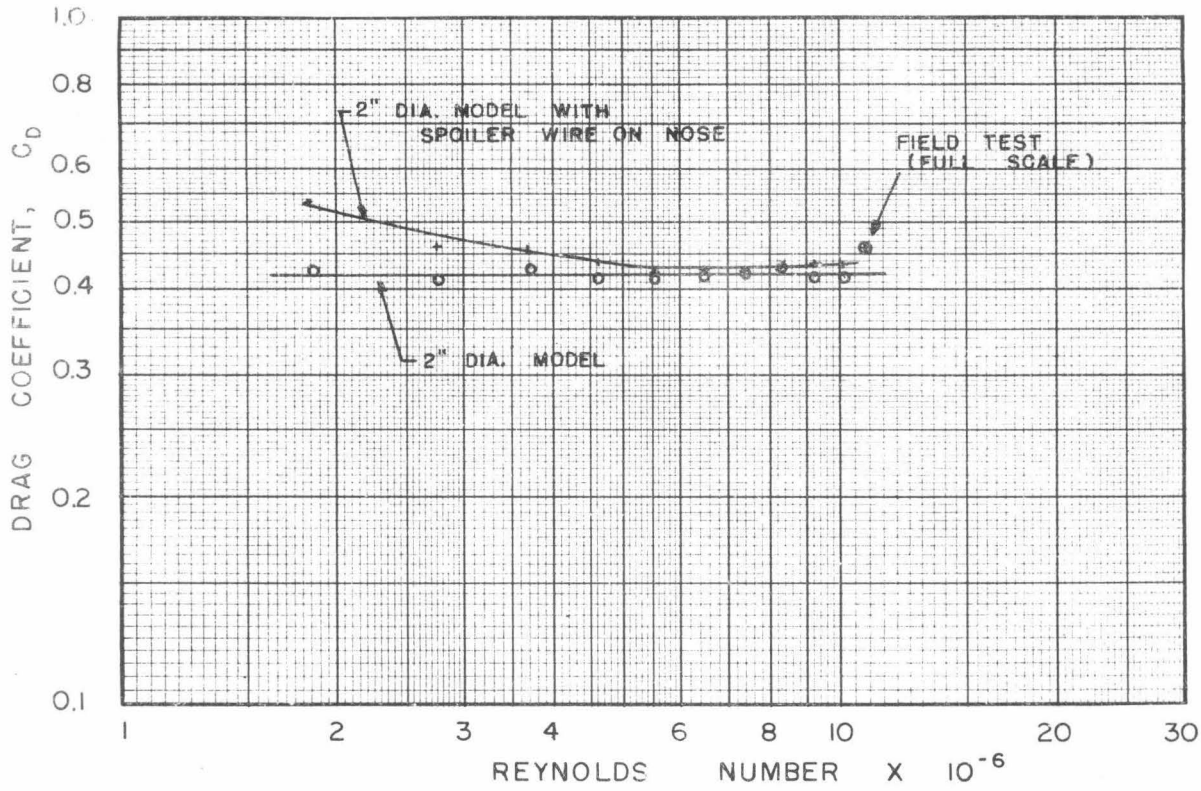


$2\frac{1}{4}$" AA ROCKET PROJECTILE

DRAG COEFFICIENT VS. REYNOLDS NUMBER
FROM WATER TUNNEL TESTS OF A
2" DIAMETER MODEL

CIT — HML
RUNS 22–25
SHEET ND 13 – 1853 L

FIGURE 6

several airfoil shapes[3] have shown that for thin airfoils, the drag at zero angle of attack increases by 10% to 15% between Mach numbers of 0.6 and 0.7. The increase occurs sooner if the airfoil is given an angle of attack. It is possible that in air the large fins of this rocket behave in a similar manner and consequently could also account for the difference between model and full scale drag.

The high drag shown by this projectile is made up of skin friction on the surface of the long body and the large fins, and of form drag, the unbalanced axial pressure distribution around the projectile. The latter, which is estimated to be from 25% to 30% of the total drag, is caused primarily by a large eddying wake behind the blunt cylindrical body. This wake is clearly shown by the flow pictures in Figure 7. These diagrams, which show the flow around the projectile at yaw angles of $0^{\circ}$, $10^{\circ}$, and $15^{\circ}$, were drawn from detailed observations of the flow in the Polarized Light Flume.*

*The Polarized Light Flume is described in Appendix A and in Reference (1).

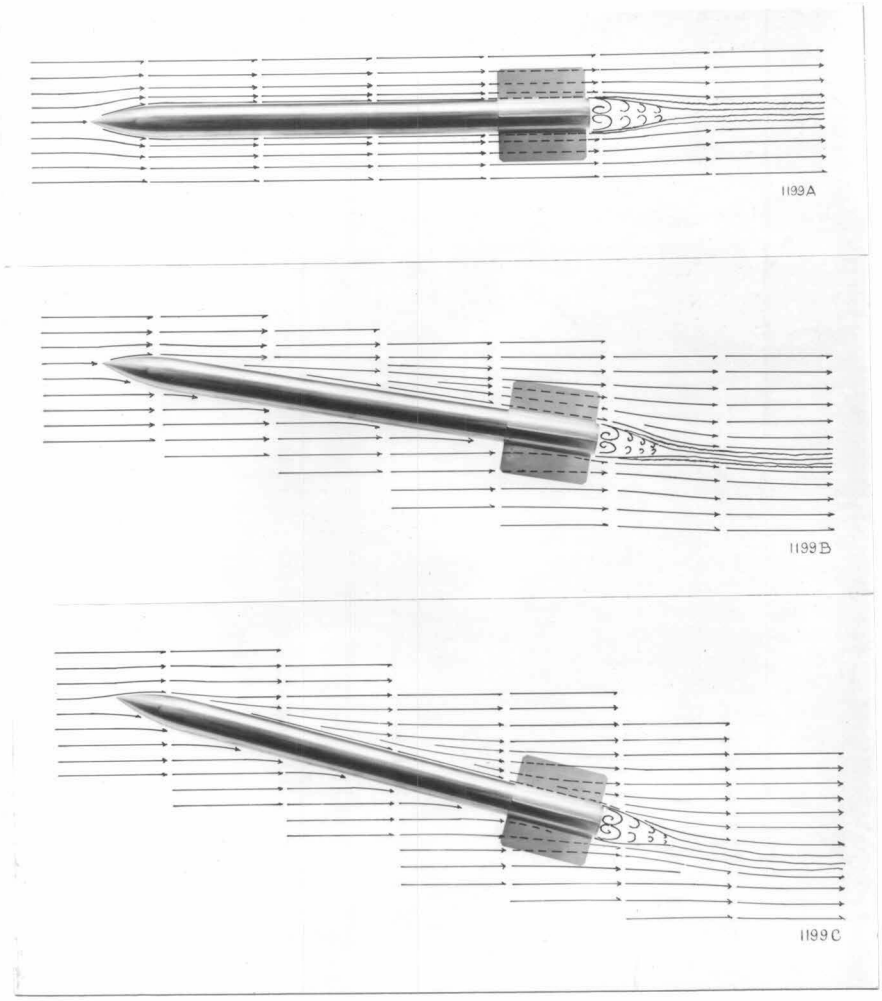


FIGURE 7

DIAGRAMS OF THE FLOW AROUND THE 2 1/4" AA ROCKET AT YAW ANGLES OF $0^{\circ}$, $10^{\circ}$, AND $15^{\circ}$. THE DIAGRAMS WERE DRAWN FROM DETAILED OBSERVATIONS OF THE FLOW PATTERN IN THE POLARIZED LIGHT FLUME.

REFERENCES:

(1) For complete description see the following report on file in the office of Section 6.1, NDRC, "The High Speed Water Tunnel at the California Institute of Technology" by R. T. Knapp, V. A. Vanoni, and J. W. Daily, June 29, 1943.

(2) Field test data, as well as Equation (1), were reported in Memorandum CIT OPC 6, "Comparison of Water Tunnel Tests on the 2-1/4" Projectile with Field Results", Leveratt Davis, Jr. to I. S. Bowen, June 12, 1943.

(3) Stack, John and von Doenhoff, Albert E. "Tests of 16 Related Airfoils at High Speeds" NACA Rep. No. 492, 1934.

# APPENDIX A

## TEST EQUIPMENT AND PROCEDURES

The tests covered by this report were conducted in the High Speed Water Tunnel at the California Institute of Technology. The following paragraphs contain a brief description of the tunnel and the test procedures employed. A more detailed description of the High Speed Water Tunnel will be found in Reference 1.

### MAIN CIRCUIT

The Water Tunnel is of the closed circuit, closed working section type. Figure A-1 shows a profile of the main flow circuit which consists essentially of the working section, the circulating pump, the stilling tank, and the necessary pipe connections. The cylindrical working section is 14" in diameter, 72" long, and is provided with three lucite windows. The propeller-type circulating pump is V-belt connected to a variable speed dynamometer. The speed of the dynamometer is automatically controlled and is held constant within ± 1 r.p.m., which corresponds to a maximum water velocity variation in the working section of 1/30 ft. per sec. While most tests are made with water velocities of 24 to 31 ft. per sec., any velocity between 10 and 72 ft. per sec. is easily obtainable.

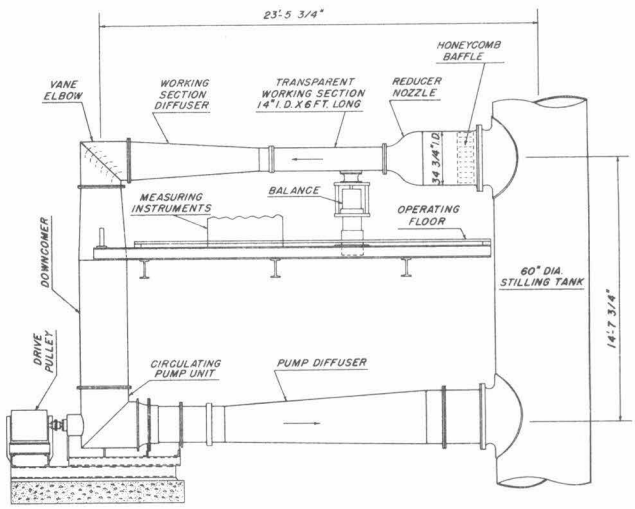


FIGURE A-1

### AUXILIARY CIRCUITS

Two auxiliary water circuits, one for pressure control and one for temperature control, are used in conjunction with the main circuit. These circuits are shown in Figure A-2, which is an isometric diagram of the complete water tunnel installation.

To make it possible to induce or inhibit cavitation at will, it is necessary that the pressure in the working section be controllable independently of the velocity. This is accomplished by superimposing the pressure regulating circuit on the main circuit.

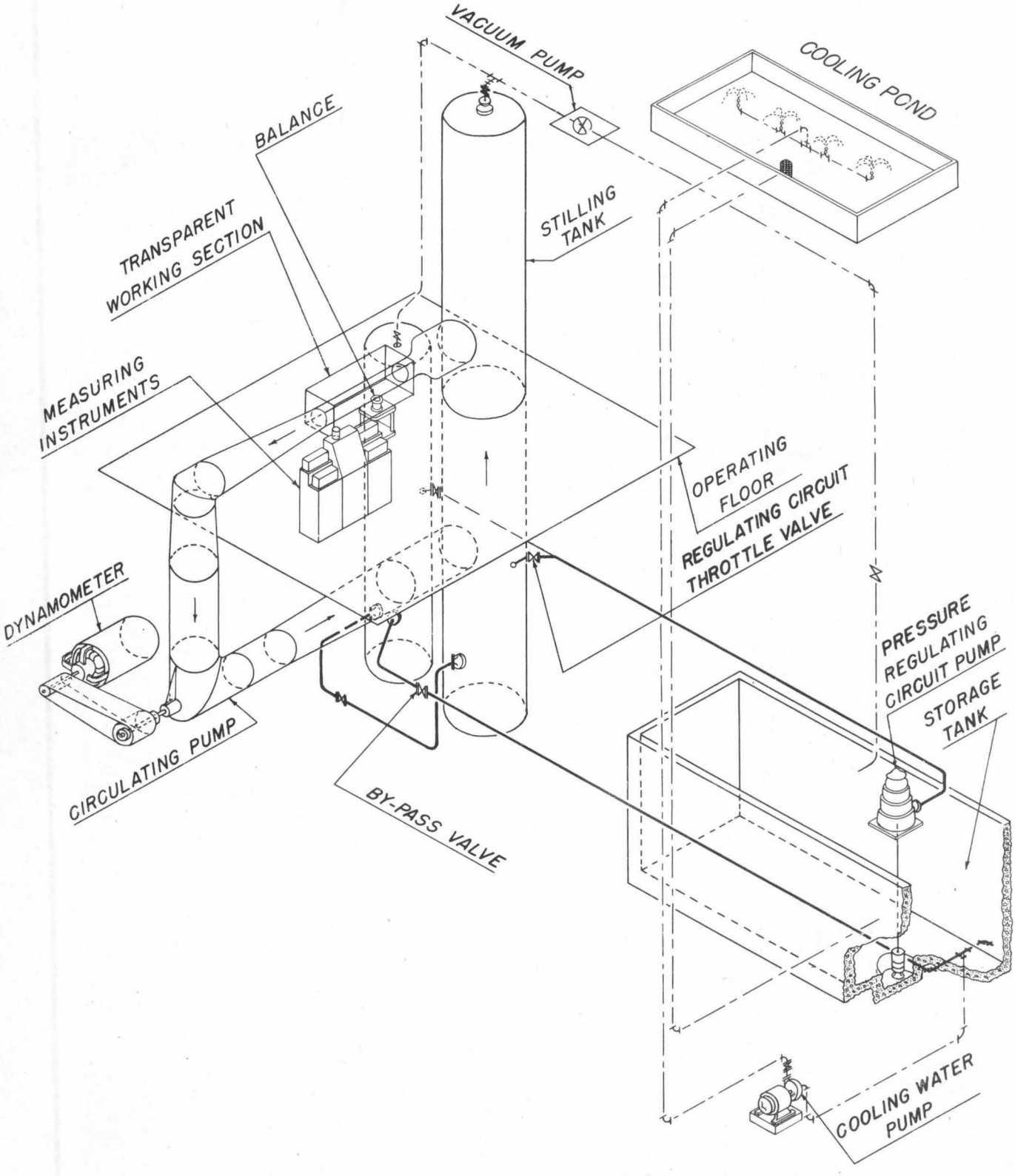
VACUUM PUMP
COOLING POND
BALANCE
STILLING TANK
TRANSPARENT WORKING SECTION
MEASURING INSTRUMENTS
OPERATING FLOOR
REGULATING CIRCUIT THROTTLE VALVE
DYNAMOMETER
PRESSURE REGULATING CIRCUIT PUMP
STORAGE TANK
CIRCULATING PUMP
BY-PASS VALVE
COOLING WATER PUMP

FIGURE A-2

A small flow of water from the sump is forced into the stilling tank by the regulating pump, and is returned to the sump through the by-pass valve. Since the main circuit is closed and completely filled, it is evident that the pressure in it may be controlled by varying the opening of the by-pass valve. A stripping pump (not shown in Figure A-2), in series with the by-pass valve, is used to produce very low pressures. The vacuum pump is used to remove air from the system so as to keep it full of water at all times.

The energy put into the water of the main circuit by the circulating pump (up to 250 HP) is all dissipated in heat. To prevent the temperature of the water from rising to undesirable values, it is necessary to remove this heat by cooling. Part of the water returned through the by-pass valve is picked up by the cooling water pump, circulated through the forced-draft cooling tower on the roof, and returned to the sump. By varying the quantity of water circulated through the cooling system, it is possible to maintain the water in the main circuit at a constant temperature.

BALANCE

The balance, shown schematically in Figure A-3, is designed to measure three components of the hydrodynamic forces acting on the model. These are the drag force parallel to the flow, the cross-force normal to the flow, and the moment around the axis of support. The three forces to be measured are transmitted hydrostatically to three self-balancing, weighing type pressure gages. These automatic gages, under glass covers, may be seen in Figure A-4, which is a view of the operating floor of the Water Tunnel. The fourth gage shown in this figure is a weighing type manometer used to determine the velocity in the working section by measuring the pressure drop across the reducing nozzle. The gages are responsive to a change in the drag or cross-force acting on the model of 0.02 pounds, and a change of 0.04 inch-pounds in the moment.

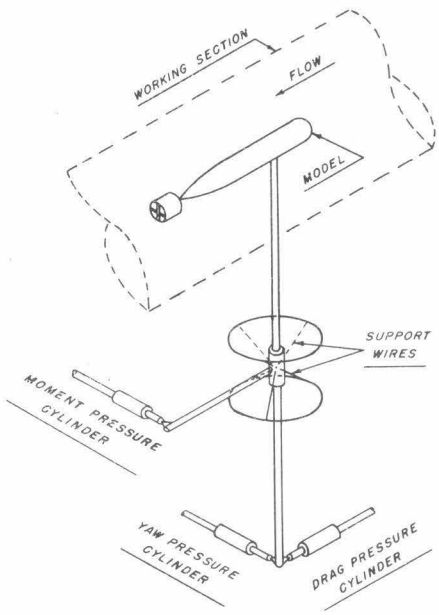


FIGURE A-3

The model is mounted on a shaft which forms the core of the vertical balance spindle shown in Figure A-3. By rotating this shaft within the spindle, it is possible to change the orientation of the model with respect to the direction of flow without altering the direction of the force components measured. Between adjustments, the spindle and shaft are held firmly together by a long, spring-loaded, tapered seat. To change the adjustment, the taper is unseated by an air diaphragm and the shaft is rotated through a worm and gear-sector by a small electric motor (not shown in the figure) mounted on the spindle. A Veeder counter on the worm gear shaft indicates the angle of attack to the nearest 1/10 degree. It should be noted that this whole system forms a part of the spindle assembly, which is pivoted about the point of intersection of the support wires. Thus it does not affect the force measurements in any way.

To reduce the drag tare to a minimum, the portion of the spindle shaft which projects into the working section is protected from the flow by a streamlined shield which extends to within a few thousandths of an inch of the model.

## POLARIZED LIGHT FLUME

The Polarized Light Flume is a separate piece of equipment used for studying the flow around submerged bodies. The fluid circulated is water containing 0.2 per cent by weight of Bentonite in suspension. Bentonite has the asymmetrical optical and physical properties required for the production of streaming double refraction. The flow to be studied is made visible by projecting a beam of light across it through a pair of polaroid plates which are oriented to produce a dark field when there is no flow. The observation section is a rectangular channel 6" wide and 12" deep, having glass sides and bottom.

The velocities used in this flume are necessarily lower than those employed in the High Speed Water Tunnel. However, this difference is not sufficient to affect the validity of the flow patterns observed. A knowledge of these flow patterns is found to be of assistance in the interpretation of the dynamic behavior of the projectiles studied. It is very helpful in investigating interference phenomena, the cause and location of separation or flow instabilities, and the behavior of the boundary layer. Care must be exercised in interpreting the observed patterns, both because the flow is three-dimensional, whereas the observed optical effect is an integration of the entire path of the light beam, and because the pattern produced is a shear pattern and not one of streamlines.

## TEST PROCEDURES

The facilities of the High Speed Water Tunnel provide for great flexibility in operation and test procedures. Individual test runs are usually made to determine the effect on the hydrodynamic forces of individual variables, although any of the variables may be changed at will independently of the others.

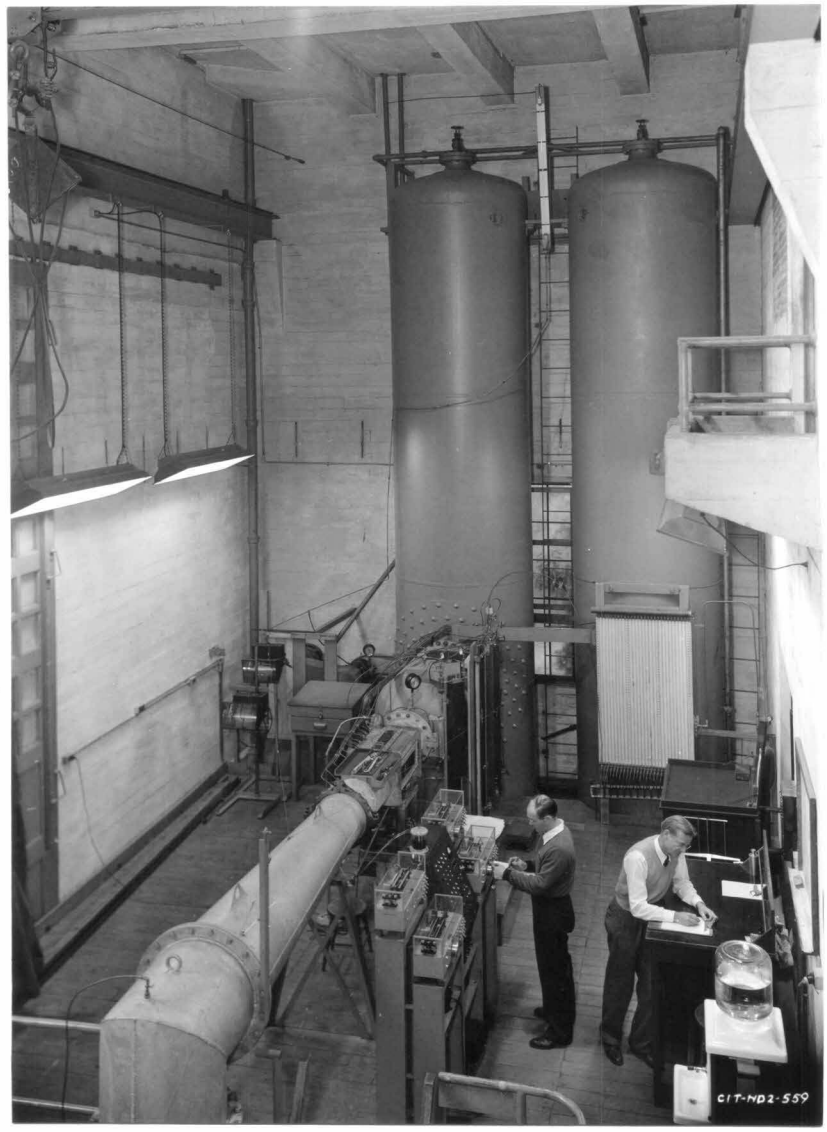


FIGURE A-4

OPERATING FLOOR
OF THE
HIGH SPEED WATER TUNNEL

Constant-velocity test runs are made to determine the variation of the hydrodynamic forces with changes in the orientation of the projectile with respect to the line of flow. The angle of attack is changed in steps of 1/2 or 1 degree, and the three force components are measured at each step.

A single test, covering the desired range of angles of attack is sufficient to completely determine the yawing characteristics of a projectile which is symmetrical about its longitudinal axis and has no movable control surfaces. A projectile which is not symmetrical about its longitudinal axis (e.g., having unequal horizontal and vertical fins) will show different characteristics when yawed in different planes and, therefore, must be tested in more than one plane. Since the model can be yawed only in a plane normal to the spindle, this is accomplished by making several separate test runs, with the model mounted on the spindle in a different orientation for each run. For instance, one run with vertical fins in a vertical position and another with horizontal fins in a vertical position. These would correspond to a yawing test and a pitching test, respectively. For a projectile with movable rudders, several tests are made, each with the rudders set at a different angle.

Cavitation is an important factor in the behavior of underwater projectiles travelling at high speed near the surface. To determine the cavitation characteristics of such a projectile, separate tests are made during which the pressure is varied while all the other factors are held constant. The inception and development of cavitation may be observed or photographed through the transparent windows of the working section, and the velocities and pressures at which cavitation begins on the various parts of the projectile are measured.

Variable-speed test runs are made to determine the scale (Reynolds number) effect on the hydrodynamic forces. The speed is usually varied in 5 fps steps and the forces are measured at each step. The pressure in the working secgion is kept high enough to suppress cavitation at the highest velocity.

# APPENDIX B

# DEFINITIONS

## YAW ANGLE

The angle, $\psi$, which the axis of the projectile makes with the direction of travel. Clockwise yaw angles are defined as positive (+) and counterclockwise angles as negative (-).

## CROSS FORCE

The hydro- or aerodynamic force, C, in pounds, exerted on the projectile in a direction normal to the line of travel. A positive cross force is defined as one acting in the same direction as the displacement of the projectile nose for a positive yaw angle.

## DRAG

The hydro- or aerodynamic force, D, in pounds, exerted on the projectile in a direction parallel with the line of travel. The drag is positive when acting in a direction opposite to the direction of travel.

## MOMENT

The hydro- or aerodynamic torque, M, tending to rotate the projectile about a transverse axis. A positive or clockwise moment tends to increase a positive yaw angle. A moment, therefore, has a destabilizing effect when it has the same sign as the yaw angle, and a stabilizing effect when of opposite sign.

## COEFFICIENTS

The force and moment coefficients are defined as follows:

Cross Force Coefficient, $C_C = \dfrac{C}{1/2\ \rho\ V^2\ A}$

Drag Coefficient, $C_D = \dfrac{D}{1/2\ \rho\ V^2\ A}$

Moment Coefficient, $C_M = \dfrac{M}{1/2\ \rho\ V^2\ A\ L}$

where

C = cross force, pounds
D = drag force, pounds
M = moment, foot-pounds

$\rho$ = density of water, slugs per cu ft

V = relative velocity between fluid and projectile, feet per second

A = area of a cross section taken normal to the longitudinal axis of the projectile at its maximum diameter, square feet

L = overall length of projectile, feet

CENTER OF PRESSURE

The point in the longitudinal axis of the projectile at which the resultant of all the hydro- and aerodynamic forces acting on the projectile is applied. This is designated by the symbol CP.

CENTER-OF-PRESSURE ECCENTRICITY

The distance between the center of pressure (CP) and the center of gravity (CG) expressed as a fraction of the length of the projectile. The center-of-pressure eccentricity, e, is defined as

$$e = \frac{L_{cg} - L_{cp}}{L} = \frac{C_{M_{cg}}}{(C \cos \psi + D \sin \psi)}$$

where

L = overall length of projectile, feet

$L_{cg}$ = distance from the projectile nose to CG, feet

$L_{cp}$ = distance from the projectile nose to CP, feet

$C_{M_{cg}}$ = moment coefficient about CG

REYNOLDS NUMBER

$$R = \frac{Vd\rho}{\mu} = \frac{Vd}{\nu}$$

where

V and $\rho$ are defined above, and

$\mu$ = absolute viscosity of water, pound-second per square foot

$\nu = \frac{\mu}{\rho}$ = kinematic viscosity of water, square feet per second

d = maximum diameter of body of projectile, feet